Kinetic Mechanism of a Partial Folding Reaction. 2. Nature of the Transition State†

Jonathan M. Goldberg and Robert L. Baldwin*

Department of Biochemistry, Beckman Center, Stanford University Medical Center, Stanford, California 94305-5307

Received September 29, 1997; Revised Manuscript Received December 29, 1997

ABSTRACT: The effects of mutations, temperature, and solvent viscosity on the bimolecular association rate constant (k_{on}) and dissociation rate constant (k_{off}) of the complex (RNaseS*) formed by S-peptide analogues and folded S-protein are reported. An important advantage of this system is that both k_{on} and k_{off} may be measured under identical strongly native conditions, and K_d for the complex may be calculated from the ratio k_{off}/k_{on} (preceding article). The side chains of S-peptide residues His-12 and Met-13 contribute a large fraction of the total interface with S-protein. Changing these residues, either singly or in a double mutant, destabilizes RNaseS* by up to 6 orders of magnitude, but causes no more than a 3-fold decrease in k_{on}. Therefore, nativelike side-chain interactions between these residues and S-protein are not present in the transition state for folding. The absence of side-chain interactions in the transition state is surprising, since it has buried 55% of the total surface area that is buried upon forming RNaseS*, as estimated from the denaturant dependences of k_{on} and k_{off} (preceding article). The temperature dependence of the refolding rate suggests that the transition state for complex formation is stabilized by hydrophobic interactions: 66% of the change in heat capacity on forming RNaseS* occurs in the association reaction, consistent with the estimate of surface area burial from the denaturant studies. The solvent viscosity is varied to determine if the folding reaction is diffusion limited. Because k_{on}, k_{off}, and K_d all can be measured under the same native conditions, the viscosity effect on reaction rates can be separated from the effect of sucrose on the stability of RNaseS*. Both k_{on} and k_{off} are found to be inversely proportional to the solvent viscosity, indicating that the association and dissociation kinetics are diffusion controlled. The stabilizing effect of sucrose on RNaseS* appears as a reduction in k_{off}.

According to transition state theory, the observed rate constant for a protein folding reaction with an exponential time course is $k_{obs} = K^{\ddagger}k^{\ddagger}$, where $K^{\ddagger}$ is the equilibrium constant for formation of the activated complex ($I^{\ddagger}$) and $k^{\ddagger}$ is the rate constant of a subsequent elementary conformational step on the folding landscape (*1*). Thus, the rate constant of a protein folding reaction gives information about $I^{\ddagger}$. The recombination and refolding reaction of the RNaseS*[1] complex formed by S-peptide analogue/S-protein can be written

$$p + N \underset{k_{off}}{\overset{k_{on}\,[S\text{-}pro]}{\rightleftharpoons}} pN \qquad (1)$$

where p is a fluorescently labeled 15-residue S-peptide analogue, N is *folded* S-protein, and pN is RNaseS*. This system has several advantages for characterizing the activated complex of a simple protein folding reaction. The equilibrium constant, K_d, for forming RNaseS* may be calculated from k_{off}/k_{on}, since the reaction is well described by the two-state approximation at S-protein concentrations below 10 μM (preceding article). k_{on} and k_{off} may be measured under identical conditions; therefore, many of the important properties of $I^{\ddagger}$ may be determined by comparing the effects of solvent additives, mutations, or temperature on k_{on} or k_{off} to those on K_d.

The slope (*m*-value) of a plot of $RT \ln X$ vs the concentration of denaturant, where X is a rate or equilibrium constant, is proportional to the number of sites for interaction with denaturant that are buried as a consequence of a folding reaction (*2*). The m-value found from k_{on} is 55% of that found from K_d, indicating that the activated complex is partially collapsed. At low salt concentrations the activated complex is stabilized by 1.4 kcal mol^{-1} from charge interactions between the negatively charged S-peptide analogue and positively charged S-protein.

Here we investigate the effects of side-chain interactions on the transition state by mutating S-peptide residues which

† This work was supported by a grant from the National Institutes of Health (GM 19988). J.M.G. was supported in part by a postdoctoral fellowship from the American Cancer Society (PF 3803). The Mass Spectrometry Facility at the University of California, San Francisco, was supported by National Institutes of Health Grant RR 01614.

* To whom correspondence should be addressed: phone, (650) 723-6168; fax, (650) 723-6783; e-mail, goldberg@cmgm.stanford.edu.

[1] Abbreviations: CspB, cold shock protein from *B. subtilis*; Pep-1, Ac−YETAAAKFERQHMDS−NH_2; Pep-1F, Pep-1 labeled via an amide linkage between N^{ϵ} of lysine-7 and the 5-carbonyl carbon of fluorescein; H12A, similar to Pep-1 except histidine-1 is replaced by alanine; H12A-1F, H12A labeled as described for Pep-1F; H12A/M13M′, similar to H12A except contains methionine sulfoxide; H12A/M13M′-1F, H12A/M′13 labeled as described for Pep-1F; M13A, similar to Pep-1 except methionine-1 is replaced by alanine; M13A-1F, M13A labeled as described for Pep-1F; Protein L, IgG binding domain of peptostreptococcal protein L; RNaseA, bovine pancreatic ribonuclease A; RNaseS, a noncovalent complex of RNaseA cleaved between residues 20 and 21; RNaseS*, a fluorescently labeled S-peptide analogue/S-protein complex; S-peptide, fragment containing residues 1−20 of RNaseS; S-protein (or S−Pro), fragment containing residues 21−124 of RNaseS.

S0006-2960(97)02403-3 CCC: $15.00
Published on Web 02/07/1998

Table 1: S-peptide Analogues

peptide	sequence[a]
S-peptide	KETAAAK FERQHM DSSTSAA
Pep−1F	ac-YETAAAK*FERQHM DS-NH_2
H12A−1F	ac-YETAAAK*FERQAM DS-NH_2
M13A−1F	ac-YETAAAK*FERQHA DS-NH_2
H12A/M13′−1F	ac-YETAAAK*FERQAM′DS-NH_2

[a] K* is the N^{ϵ}, 5-carboxyfluorescein amide of lysine. M′ is the sulfoxide of methionine.

are known to be important in stabilizing RNase S (*3*). The relatively small size of the interface between S-peptide and S-protein allows us to disrupt approximately half of the total nonpolar side-chain interaction area by replacing the side chains of His-12 and Met-13 with Ala, either singly or in a double variant with Ala in position 12 and methionine sulfoxide in position 13. Nonlinear Arrhenius plots of ln k vs $1/T$, where k is the rate constant of a protein folding reaction, reflect the difference in the heat capacity (ΔC_p) between the reactants and the transition state (*4*, *5*). The positive ΔC_p observed for protein unfolding reactions results chiefly from exposure of hydrophobic surface area (ref 6 and references therein). A comparison between the temperature dependence of k_{on} or k_{off} with that of K_d is therefore expected to measure the extent to which hydrophobic interactions present in RNaseS* are formed in the transition state. The relatively small size of the folding unit (15 residues) makes it less likely that any nonlinear temperature dependence results from escape from kinetic traps (*7*).

While denaturants and mutations affect the stability of the activated complex, viscosity-increasing reagents such as sucrose affect both the stability of $I^{\ddagger}$ and the value of the kinetic prefactor, $k^{\ddagger}$. Whether the protein folding process is diffusion-limited is a long-standing question (*8*), but the complex effects of viscosity-increasing reagents have made interpretation of the kinetic data difficult (*9*, *10*). The RNaseS* system allows k_{on} and k_{off} to be measured independently under identical native conditions, allowing the effects of sucrose on $K^{\ddagger}$ and $k^{\ddagger}$ to be separated.

MATERIALS AND METHODS

Materials. S-protein and S-peptide analogues were prepared as described in the preceding article. The sequences of the peptides used in this study are given in Table 1. H12A-1F was found by fast atom bombardment mass spectrometry (Mass Spectrometry Facility, University of California, San Francisco) to be oxidized to the form containing methionine-13 sulfoxide (H12A/M13M′-1F). H12A/M13M′-1F was reduced to H12A-1F as follows: 2 mg of the oxidized analogue was dissolved in 1 mL of sparged water, and argon was blown over the sample for 1 min. The sample was incubated in a closed container at room temperature for 68 h after addition of 100 μL of β-mercaptoethanol. The sample was lyophilized, dissolved in 1 mL of 10 mM ammonium acetate buffer, pH 6.8, 15% acetonitrile, filtered, and purified by fast protein liquid chromatography (FPLC) chromatography as previously described (preceding article). The yield of >95% pure H12A-1F was 60%.

Kinetic Measurements. The visible absorbance and emission spectra of S-peptide analogues labeled with fluorescein at Lys-7 change on complex formation with S-protein, which provides a sensitive assay for complex formation (preceding article). The bimolecular association rate constant, k_{on}, is determined by following the time course of fluorescence emission after mixing a labeled S-peptide analogue with S-protein in a stopped flow spectrophotometer, and the dissociation of RNaseS* (described by k_{off}) is measured after adding a large excess of unlabeled S-peptide analogue. The excitation wavelength was 496 nm throughout, and the other details are described in the preceding article. The solvent viscosity was varied by adding either 0.399, 0.632, 0.842, or 0.988 M sucrose, corresponding to relative solvent viscosities of 1.48, 1.94, 2.57, and 3.18, respectively (*11*).

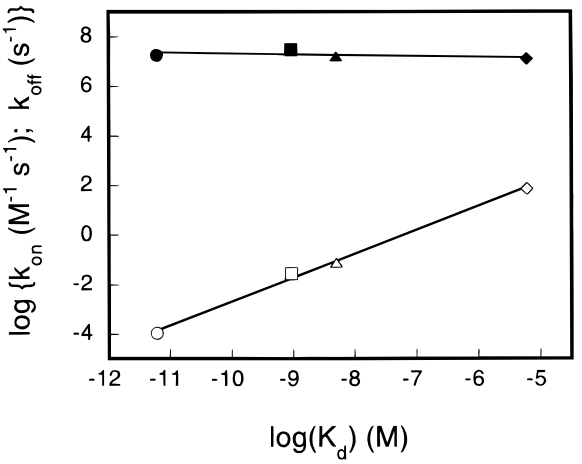

FIGURE 1: Effects of various side chains (see Table 1) on the kinetic and equilibrium parameters for formation of the RNaseS* complex. The logarithms of k_{on} (filled symbols) and k_{off} (open symbols) are plotted against the logarithm of K_d ($K_d = k_{off}/k_{on}$) for (●,○) Pep-1F, (■,□) H12A-1F, (▲,△) M13A-1F, and (◆,◇) H12A/M13M′-1F, where M′ is methionine sulfoxide. The value of the slope (times −1) of the line through the k_{on} data gives ϕ (*19*) and has a value of 0.03 ± 0.04. Kinetics are measured by fluorescence emission with an excitation wavelength at 496 nm at 10 °C in 10 mM MOPS, pH 6.7. For k_{on} the concentrations of labeled S-peptide analogues are 0.1−0.4 μM, and the S-protein concentrations are 2−10 μM. For k_{off} the labeled S-peptide concentrations are 0.1−1 μM with a 2-fold excess of S-protein, and the concentrations of Pep-1 (unlabeled) are 50−500 μM.

RESULTS

Effects of Mutations. The bimolecular association rate constant (k_{on}) and dissociation constant (k_{off}) were measured for Pep-1F and the following mutant peptides (see Table 1): H12A-1F, M13A-1F, and H12A/M13M′-1F, where M′ is methionine sulfoxide. The results are plotted against the logarithm of K_d ($K_d = k_{off}/k_{on}$) in Figure 1. The mutant RNaseS* complexes span a stability range of 6 orders of magnitude. The value of k_{on} is nearly constant over the entire range of K_d. The entire effect on stability comes from an increase in k_{off}.

Temperature Dependence of the Kinetic Parameters. Arrhenius plots of k_{on} and k_{off} for Pep-1F and M13A-1F in 10 mM MOPS, pH 6.7, are shown in parts a and b of Figure 2, respectively. The value of k_{on} was calculated using the total S-protein concentration after correction for the small fraction of unfolded S-protein present at the upper end of the temperature range (*12*). The Arrhenius plot of k_{on} displays considerable downward curvature and k_{on} varies by less than an order of magnitude between 1 and 30 °C, while the Arrhenius plot for k_{off} displays a small but significant

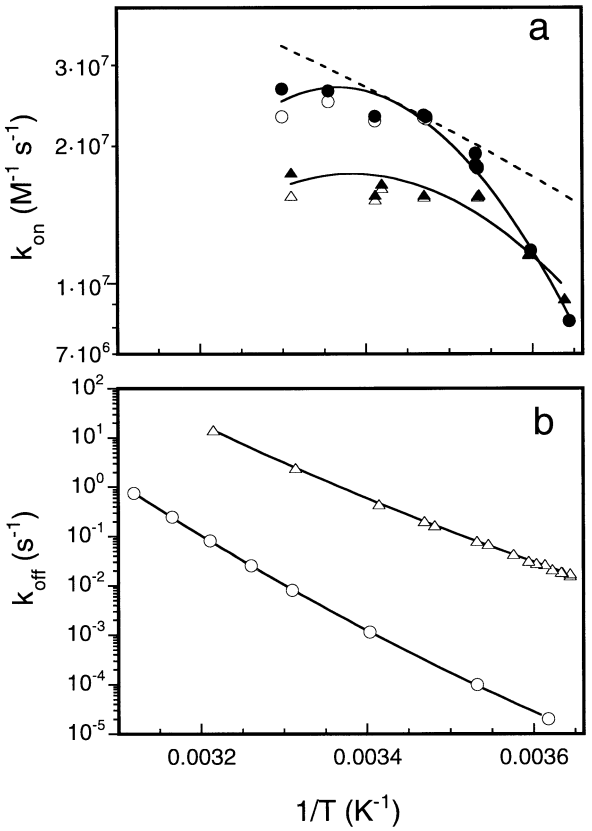

FIGURE 2: Dependence on temperature of the association and dissociation rate constants for forming RNaseS*. The conditions are the same as those described in Figure 1, except the temperature varies from 1.3 to 30 °C. (a) k_{on} for (●,○) Pep-1F and (▲,△) M13A-1F. The open symbols are the values calculated by the linear method described in Figure 3 of the preceding article, and the closed symbols are these values corrected for the unfolded fraction of S-protein (*12*). The solid lines are obtained from fits of eq 2 to the corrected values (Table 2). The dotted line shows the expected effect of temperature on an encounter-limited reaction; its rate depends chiefly on the diffusion coefficients of the reactants and thus on the viscosity of water. The curve is arbitrarily drawn through the Pep-1F datum at $(1/T) = 0.00347$ K^{-1}. (b) k_{off} for (○) Pep-1F and (△), M13A-1F. The solid lines are calculated as described above for k_{on}.

upward curvature and k_{off} varies by several orders of magnitude. The value of k_{on} is identical for Pep-1F and M13A-1F at 5 °C, but Pep-1F associates with S-protein 1.5-fold more rapidly at 25 °C. k_{off} is always more than 2 orders of magnitude smaller for Pep-1F than for M13A-1F.

The temperature dependence of the kinetic data was modeled using a rearrangement of the equation of Chen et al. (*13*)

$$\ln k = (R \ln k^{\ddagger} + \Delta S^{\ddagger}_{ref})/R - (1/RT)\{\Delta H^{\ddagger}_{ref} - \Delta C_p{}^{\ddagger}[T - T_{ref} - T \ln(T/T_{ref})]\} \quad (2)$$

which assumes that the observed rate constant is the product of the equilibrium constant, $K^{\ddagger}$, for forming the activated complex, and a kinetic prefactor, $k^{\ddagger}$. The parameters $\Delta S^{\ddagger}_{ref}$ and $\Delta H^{\ddagger}_{ref}$ at $T_{ref} = 283.15$ and $\Delta C_p{}^{\ddagger}$ (assumed to be independent of temperature between 0 and 30 °C) are thermodynamic parameters for the equilibrium between the reactants (p + N in refolding and pN in unfolding, eq 1) and the activated complex, $I^{\ddagger}$. The value of the prefactor, $k^{\ddagger}$, is unknown, and R ln $k^{\ddagger}$ is inseparable from $\Delta S^{\ddagger}_{ref}$ by our methods. Therefore we fitted eq 2 to our data using the parameter $\Delta S_{app} = R \ln k^{\ddagger} + \Delta S^{\ddagger}_{ref}$. Fortunately, the term $R \ln k^{\ddagger}$ cancels when the equilibrium constant is calculated from the rate constants and also in other comparisons between rate constants. The cancellation of $R \ln k^{\ddagger}$ is a consequence of microscopic reversibility since k_{on} and k_{off} are measured under identical conditions. The values of the thermodynamic parameters from the best fit of eq 2 to the data in Figure 2, and the equilibrium parameters calculated from them, are given in Table 2. The best fit parameters in Table 2 were used to calculate the values of k_{on} and k_{off} over a range of temperatures, and the ΔG value for overall folding [$\Delta G = -RT \ln(k_{on}/k_{off})$] is plotted in Figure 3. Data points are included in Figure 3 when k_{off} and k_{on} are measured within 1 degree of each other.

Comparison of the Kinetically Determined Thermodynamic Parameters with Those Measured by an Equilibrium Method. The thermodynamics of binding of shortened S-peptide (S-15) to S-protein have been characterized by titration microcalorimetry (*14*). Pep-1F binds more strongly to S-protein than does S-15 for the reasons discussed in the preceding article. The decrease in the stability of RNaseS* caused by the M13A mutation is, however, identical whether starting with Pep-1F or S-15 (Table 2). The temperature dependence of K_d is qualitatively similar for all the analogues (Figure 3). The value of ΔC_p for the equilibrium reaction, calculated from k_{off}/k_{on}, should equal that measured by titration microcalorimetry, as observed for Pep-1F and S-15 (Table 2). The value of ΔC_p for the M13A-1F variant calculated from our data is significantly smaller, however, than the directly measured value for M13A in the S-15 background, and we have no explanation for this discrepancy. The value of $\Delta\Delta C_p$ caused by the M13A mutation in the Pep-1F background is -0.42 ± 0.18 kcal mol^{-1} K^{-1} (Table 2), in poor agreement with the predicted value of -0.019 kcal mol^{-1} K^{-1} (see ref 14, for a discussion of similar discrepancies).

Viscosity Effects. The viscosity effect is given here as the slope of a plot of k_0/k_η against the relative viscosity η/η_0, where k_0 is the rate constant at a relative viscosity of 1 and k_η is the rate constant at elevated relative viscosity. A slope of 1 indicates a diffusion-limited reaction and a slope of zero indicates a reaction which is not diffusion limited, if there is no effect of the viscosogenic cosolvent on the folding or unfolding rate constant arising from a change in the stability of the folded protein (*9*, *10*, *15*, *16*). There are significant viscosity effects (with sucrose) on k_{on} and k_{off} for the reaction of Pep-1F and S-protein at 10 °C in 10 mM MOPS, pH 6.7 (Figure 4). A slope close to 1 is observed for refolding, and separation of the viscosity and stability effects on k_{off} is considered in the Discussion. The scatter in the k_{off} data is the result of instrumental drift and possible sample degradation during the long data acquisition times which are required. The effects on k_{on} of adding 0.1 M NaCl or of substituting M13A-1F for Pep-1F are measured at a single elevated viscosity; the results are like those for Pep-1F described above (Figure 4).

DISCUSSION

The Activated Complex is not Stabilized by Nativelike Side-Chain Interactions. A model for the docking of S-peptide with S-protein is obtained by constructing solvent acces-

Table 2: Thermodynamic Parameters for RNaseS* and Other S-protein/S-peptide Analogue Complexes[a]

	Pep1F			S−15
	association	dissociation	equilibrium[b]	equilibrium[c]
ΔH (kcal mol^{-1})	9.9 ± 0.6	36.8 ± 0.4	−26.9 ± 0.8	−27.5 ± 0.6
ΔS (kcal mol^{-1} K^{-1})	0.068[d] ± 0.003	0.111[d] ± 0.001	−0.043 ± 0.004	−0.063[e] ± 0.007
ΔC_p (kcal mol^{-1} K^{-1})	−0.71 ± 0.09	0.37 ± 0.02	−1.08 ± 0.10	−0.91 ± 0.10
ΔG (kcal mol^{-1})			−14.5 ± 0.1	−9.8[e] ± 1.8
	M13A−1F			S−15/M13A
	association	dissociation	equilibrium[b]	equilibrium[c]
ΔH (kcal mol^{-1})	5.2 ± 0.9	28.9 ± 0.3	−24 ± 1	−21.3 ± 0.6
ΔS (kcal mol^{-1} K^{-1})	0.051[d] ± 0.004	0.097[d] ± 0.001	−0.046 ± 0.005	−0.053 ± 0.002
ΔC_p (kcal mol^{-1}K^{-1})	−0.42 ± 0.14	0.27 ± 0.03	−0.66 ± 0.15	−0.96 ± 0.08
ΔG (kcal mol^{-1})			−10.9 ± 0.1	−6.2 ± 0.1

[a] The conditions are T = 10 °C, 10 mM MOPS, pH 6.7 ± 0.1 except where noted. The kinetic parameters are obtained from a fit to the data in Figure 2 of eq 2, with T_{ref} = 283.15 K. [b] The equilibrium parameters are calculated from the kinetic parameters, and $\Delta G = -RT \ln(k_{off}/k_{on})$ at 10 ± 0.3 °C. [c] Titration calorimetry data from ref *14*. The conditions are 50 mM sodium acetate, 100 mM NaCl, pH 6.0. S-15 = NH_2−KETAAAFERQHMDS−OH and S-15/M13A is the analogue where M13 is replaced with A. ΔS at 10 °C is calculated from $(\Delta H_{10\,°C} - \Delta G_{10\,°C})$/283.15 K. [d] $\Delta S_{app} = R \ln k^{\ddagger} + \Delta S^{\ddagger}_{ref}$, where $k^{\ddagger}$ is the transition prefactor (see text). [e] Extrapolated from titrations at higher temperature with eq 5 of ref *14*.

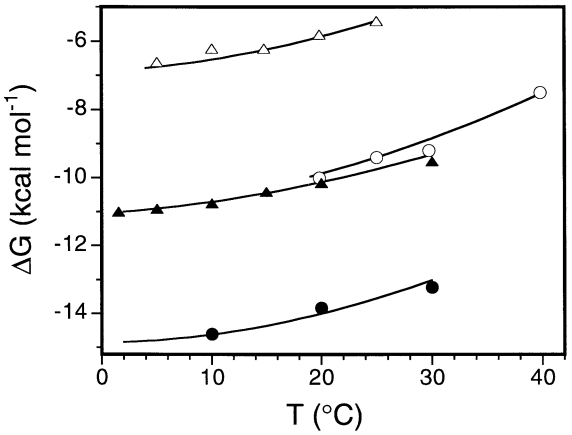

FIGURE 3: Temperature dependence of the stability ($\Delta G = RT \ln K_d$) of RNaseS* complexes: filled symbols, our data with conditions as described in Figure 1 except for the variation in temperature; open symbols, titration calorimetry data of Varadarajan et al. (*14*) in 50 mM sodium acetate, 100 mM NaCl, pH 6. Stabilities of (●) Pep-1F, (○) S-15 (the first 15 residues of S-peptide), (▲), M13A-1F, and (△), S-15/M13A. The lines through our data are calculated from $K_d = k_{off}/k_{on}$ where k_{off} and k_{on} are calculated from eq 2 with the best fit parameters in Table 2. Data points are included only when k_{off} and k_{on} are measured at temperatures within 1 degree of each other. The lines through the data of Varadarajan et al. (*14*) are calculated from their eq 5, using parameters from their Tables 1 and 2.

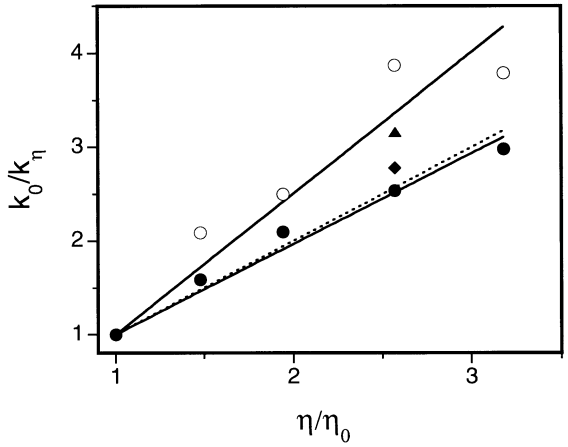

FIGURE 4: Dependence on viscosity of the association and the dissociation rate constants for forming RNaseS* complexes. η/η_0 is the ratio of the solvent viscosities in the presence and absence of sucrose, and k_0/k_η is the ratio of the rate constants in the absence and presence of sucrose. The slope of the plot is 1 for a completely diffusion-limited reaction (dashed line) and 0 for a reaction which is not diffusion limited. The conditions are as described in Figure 1 except for the presence of sucrose, or as otherwise noted. k_{on} for (●) Pep-1F, (◆) Pep-1F with 0.1 M NaCl, and (▲), M13A-1F. k_{off} for Pep-1F (○). The solid lines are linear fits of k_{on} and k_{off} for Pep-1F in the absence of NaCl and are constrained to pass through (1,1). Their slopes are 0.97 ± 0.05 and 1.5 ± 0.2, respectively.

sibility surfaces around the S-peptide and S-protein moieties in the X-ray structure of RNase S (*17*). Such a model reveals a distinct hydrophobic pocket whose sides are in van der Waals contact with the side chains of F8, H12 and M13. The change in accessible nonpolar surface area upon forming RNaseS that involve S-peptide side chains is estimated to be 550 Å^2 (*18*).[2] The side chains of H12, and M13 contribute 105 and 180 Å^2 to this amount, respectively. Therefore, the mutations of H12 and M13 described below disrupt roughly half the nonpolar side-chain interactions stabilizing RNaseS*. The total change in solvent-accessible surface area for forming RNaseS from extended S-peptide and folded S-protein involves burial of 1230 Å^2 of nonpolar surface area and 990 Å^2 of polar surface area.

[2] The absolute values of the solvent accessibility changes are uncertain; the relative amounts are expected to be more accurate.

The H12, M13A, and H12A/M13-sulfoxide variants increase K_d (weaken binding) by up to 6 orders of magnitude (Figure 1), underscoring the importance of these side chains to complex stability. To what extent do these interactions stabilize the transition state? The mutations reduce k_{on} by only 3-fold over the entire range of complex stability; almost the entire effect on stability comes from increases in k_{off}. Therefore, specific interactions of H12 and M13 are not present in the activated complex. We have not varied every side chain at the interface between S-peptide and S-protein, but considering the large fraction of the total interaction area disrupted by the H12A/M13-sulfoxide variant, the wide range of complex stabilities investigated, and the linearity of the plot of ln k_{on} vs ln K_d over this range, we expect that no specific side-chain interactions are present in the activated complex.

The ratio $-\Delta \ln k_{on}/\Delta \ln K_d$ is defined as the ϕ-value of a mutation (*19*): $\phi = 1$ means that the residue stabilizes the transition state as much as it does the native protein, and $\phi = 0$ means that the residue stabilizes the transition state not at all. The average ϕ-value for RNaseS* complex formation is 0.03. The low ϕ-values might be rationalized from the fact that the binding site on S-protein is preformed. This structured site allows favorable contact interactions to be made on binding without an associated unfavorable change in the conformational entropy of S-protein. Thus, any complex containing a nativelike side-chain interaction will have a lower free energy than that of the activated complex and will equilibrate with pN. What is surprising, however, is the absence of side-chain interactions in a transition state that is significantly collapsed: 55% of the total surface area for complex formation is buried in the activated complex, as inferred from comparing the *m*-values of k_{on} and K_d (preceding article).

Is the Transition State Stabilized by α-Helix Formation? S-peptide is helical between residues 3 and 13 in RNaseS, raising the possibility that the transition state is stabilized by α-helix formation. The presence of α-helix could explain why $I^{\ddagger}$ is collapsed and lacks specific side-chain interactions. The role of helix formation in RNaseS* complex formation is unknown and must be tested in future work by characterizing mutants which specifically destabilize the helix. It may be inferred from a previous study that the helix is not fully stable in the activated complex (*20*). Tritium washes out from the helical region of S-peptide bound to S-protein from an intermediate that is in equilibrium with the folded complex, indicating that the helix is substantially unfolded before it dissociates. The principle of microscopic reversibility implies that the helix is not fully stable until after it associates with S-protein.

Surprisingly, widespread helix formation is not present in the transition state for the refolding of the GCN4-p1 coiled-coil (*21*). Ala to Gly mutations at solvent exposed sites destabilize the two individual helixes without affecting nonpolar packing interactions at the dimer interface. These mutations significantly destabilize the coiled-coil but have relatively little effect on k_{on}, suggesting that the helixes are not present in the activated complex. This behavior suggests a mechanism where folding initiates anywhere along the coiled-coil interface, thereby bypassing the mutation site, but it is difficult to reconcile this mechanism with the *m*-value from the refolding rate constant, which is 55% of the total for the folded coiled-coil.

Source of the Curvature in Arrhenius Plots of the Rate Constants. The curvature in Arrhenius plots of k_{on} and k_{off} vs $1/T$ (Figure 2) may be explained in different ways: (a) a change in heat capacity (ΔC_p) which is predominantly the result of burial of apolar surface area in the activated complex (*4*, *6*); (b) a change in the rate-determining step; (c) escape from kinetic traps (*7*). We have not ruled out the latter two explanations for the observed temperature dependence, but the simplicity of the reaction between S-peptide and folded S-protein makes them less likely than for the folding reactions of larger proteins. By plotting data for the temperature dependence of the refolding rate at constant stability, with the aid of measurements made at varying denaturant concentrations and temperatures, Scalley and Baker (*5*) showed that ΔC_p accounts for most of the curvature in the data for two proteins, CspB and protein L. We assume that the curvature in plots of $\ln k_{on}$ vs $1/T$ also results from a decrease in ΔC_p in the activated complex.

The Transition State Is Stabilized by Nonspecific Hydrophobic Interactions. If specific side-chain interactions do not stabilize the transition barrier species for forming the RNaseS* complex, then what types of interactions do? Most (66%) of the total decrease in heat capacity upon forming pN from p and N occurs in the refolding reaction (Table 2). This indicates that over half of the total hydrophobic surface area that is lost upon forming RNaseS* is already buried in the transition state. Since hydrophobic surface area burial is a favorable process under our experimental conditions, it follows that the activated complex is stabilized by hydrophobic interactions. The large activation enthalpy of k_{off} (Figure 2, Table 2) indicates that most of the enthalpic interactions that stabilize RNaseS* are absent in the transition state. The relatively small increase in ΔC_p found from k_{off} (34% of the total for RNaseS*) indicates that breaking these bonds is not accompanied by a large increase in solvation. Breaking specific van der Waals contacts between side chains probably accounts for a large part of the activation enthalpy found from k_{off}. This interpretation is supported by the observation that replacing buried side chains with Ala produces large increases in k_{off} and small decreases in k_{on} (Figure 1).

The temperature dependences of the refolding and unfolding rate constants of the RNaseS* complex are similar to those of several small single-chain proteins (*13*, *22*−*25*). The universality of this behavior suggests that transition states for protein folding are generally collapsed and stabilized by hydrophobic interactions. The new information provided by this study is that this temperature dependence can occur without specific side-chain interactions.

Comparison between ΔC_p and m-values as Measures of Surface Area Exposure in the Transition State. ΔC_p and the *m*-value are both thought to reflect the extent of surface area burial associated with protein folding (*26*). The Zwanzig (*27*) model for protein folding predicts that the transition barrier species become more structured as the denaturant concentration is increased. In this model denaturants do not affect the unfavorable conformational entropy cost of folding, but they do reduce the favorable free-energy change associated with forming native residue conformations. This means that a greater number of correctly oriented residues, that is, a more buried transition state, is required to provide enough free energy to overcome the conformational entropy barrier opposing folding (*1*). Thus, the extent of solvent exposure of the transition state measured from kinetic *m*-values may depend on denaturant concentration, and measurements of *m*-values and ΔC_p may give different estimates of the extent of surface burial. This problem is minimized by measuring the kinetic *m*-values for folding and unfolding under identical conditions at low denaturant concentrations, as we have done. The predicted extent of surface area burial in the transition barrier for RNaseS* is 0.66 ± 0.1 based on ΔC_p (Table 2), which differs slightly from the value of 0.54 ± 0.04 based on the *m*-values for k_{on} and K_d in urea (preceding article). A possible explanation for this discrepancy is that hydrophobic surface area burial is not the sole determinant either of ΔC_p or of the m-value, and burial of polar groups has different effects on ΔC_p and on the *m*-value.

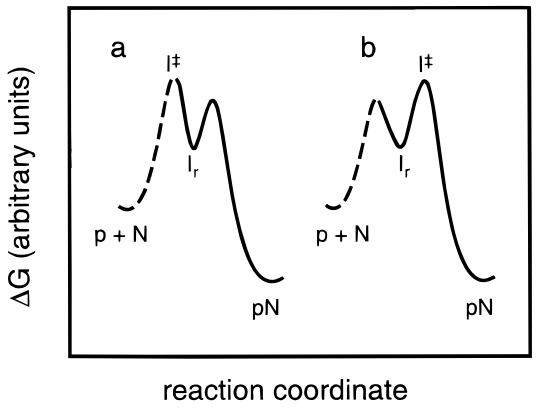

FIGURE 5: Free energy profiles for the formation and dissociation of RNaseS*: (a) for an encounter-limited reaction with I_r occurring after the rate-determining state and (b) for a folding-limited reaction with a I_r occurring as a preequilibrium intermediate before the rate-determining step. The rate-determining steps are indicated by I‡. The heights of the first barriers are shown as dashed lines since they depend on the concentrations of the reactants.

Is the Reaction Encounter-Limited or Folding-Limited? The viscosity effects of 0.97 for k_{on} and 1.5 for k_{off}, measured under identical native conditions (Figure 4), indicate that the reaction is diffusion-limited and that sucrose stabilizes the complex. The effect of sucrose on the stability of RNaseS* is obtained from the dependence of K_d on sucrose concentration ($-RT\ \Delta \ln K_d/\Delta$[sucrose] $= -0.20 \pm 0.08$ kcal mol^{-1} M^{-1}, assuming a linear model). If the stability effect is assigned to k_{off}, then both k_{on} and k_{off} have viscosity effects close to 1, indicating that the folding reaction is fully diffusion-limited. This means that forming the transition state involves the diffusion together and collision of protein groups and that the protein−sucrose interactions stabilizing the complex are not present in the transition state. Moreover, it implies that folding of RNaseS* may be modeled using diffusion-collision theory (*8*). The important issue of whether the reaction is encounter-limited or folding-limited is unresolved, however.

Every encounter between correctly oriented reactants leads to product in an encounter-limited bimolecular reaction, and the forward and reverse rate constants for such a reaction are inversely proportional to the solvent viscosity (*28*, *29*). Unimolecular reactions of proteins and peptides may also be diffusion-limited (*9*, *10*, *30*−*33*) and a reaction which follows bimolecular kinetics may have a bimolecular preequilibrium step followed by a rate-limiting unimolecular step. Therefore, it is not possible to conclude that a bimolecular reaction involving a protein folding reaction is encounter-limited, even if it has an inverse dependence on the solvent viscosity.

The available data do not decide whether the highest point on the free energy profile for RNaseS* formation occurs upon the encounter of reactants (Figure 5a) or occurs after formation of an encounter complex (I_r in Figure 5b). Arguments in favor of an encounter-limited mechanism are as follows. (a) Collision of the reactants is a nonspecific process, and the low ϕ-values for mutations which destabilize the complex (Figure 1) indicate that the transition barrier species are not stabilized by specific side-chain interactions. Low ϕ-values have also been observed for the refolding of the GCN4-p1 coiled-coil (*21*), as discussed above. (b) The effect of solvent viscosity on RNaseS* formation is near unity at low relative viscosities (Figure 4), and a similar effect has been measured for the MYL arc repressor dimer (*34*). This behavior indicates that the internal friction is small at the free energy barrier for refolding, where the internal friction is defined as the resistance to conformational change from sources other than solvent (*33*). Internal friction has been measured in experiments on the diffusion of peptide ends relative to each other, and the results show that, to have low internal friction, the motions carrying polypeptide chains across the transition barrier must involve segments of more than 5 residues (*31*). A rate-limiting step within the encounter complex involving residues separated by more than five peptide groups is difficult to visualize for S-peptide binding to the folded S-protein. (c) Polyol compounds such as sucrose stabilize folded proteins (*15*, *16*). k_{on} and k_{off} are measured here under identical conditions, which allows the effect of sucrose on the stability of the complex to be separated from its viscosity effect on the kinetics. The stabilizing effect of sucrose on RNaseS* can be assigned to an effect on k_{off} (see above). This assignment suggests that little surface area is buried in the transition state, as expected for an encounter-limited reaction. The assignment contradicts, however, the conclusion from the temperature and denaturant dependences and suggests that different kinds of surface are involved in these two cases. The stabilizing effects of polyol compounds on the folding of single-chain proteins appear mainly in the refolding reaction, thus tending to cancel the viscosity effect on the refolding kinetics (*9*, *10*).

There are also several good arguments for concluding that the RNaseS* folding reaction should be folding-limited (Figure 5b). (a) An encounter complex is not expected to be desolvated (*35*) and should not be stabilized by hydrophobic interactions or hydrogen bonds between the reactants. Thus, k_{on} should be nearly independent of the denaturant concentration, since the effect of urea on the solvent viscosity is small (*11*). We observe a significant effect of denaturants on k_{on}, however (preceding article). (b) Likewise, the temperature dependence of k_{on} is inconsistent with that expected for an encounter-limited reaction; there is more curvature in the Arrhenius plot of the experimental refolding data than expected for a hypothetical encounter-limited reaction (Figure 2a, dashed line), whose temperature dependence should stem from changes in the viscosity of water. The substantial ΔC_p found in the refolding reaction suggests that the activated complex is partially desolvated. (c) The leveling-off of k_{obs} for refolding above 10 μM S-protein may be the result of forming of a preequilibrium intermediate before the rate-determining step in folding (see preceding article). The existence of such an intermediate would be incompatible with an encounter-limited mechanism. (d) Janin (*35*) concluded that the association reactions occurring between two fully folded protein molecules are not likely to be encounter-limited. Forming the transition state involves a free energy barrier of from 6.7 to 8.5 kcal mol^{-1} resulting from a loss rotational entropy at 10 °C, which places the rate-determining step after formation of the encounter complex. For a 15-residue peptide, the free-energy change upon ordering the backbone is about 14 kcal mol^{-1} at 10 °C (*36*). It would be surprising if the formation of RNaseS* is encounter-limited, when the simpler process of association of folded protein molecules is not.

The resolution of this important ambiguity may be resolved by characterizing the intermediate (I_r) on the refolding pathway that is populated at S-protein concentrations above 10 μM (preceding article) and by studying the folding reactions of mutant S-peptide analogues in which the helix is destabilized. Either outcome will have important implications. If the process is encounter-limited, then the current theoretical view of such reactions (*35*) must be enlarged to describe the effects of temperature and denaturants. The refolding of S-peptide would have to take place at least 5 times faster than the dissociation of the encounter complex if this model is correct. On the other hand, if the rate-determining step occurs after formation of an encounter complex, then the I_r intermediate must be collapsed but not stabilized by specific side-chain interactions. Such an intermediate would be similar to the early collapsed forms of proteins which occur during refolding (*37, 38*), to the protein aggregates which are formed rapidly in the refolding reactions of some small proteins (*39*), and to complexes formed between unfolded proteins and chaperonins. Finally, I_r would fall under the definition of a molten globule intermediate (*40*), if future studies find it to be significantly helical.

An Emerging Description of the Transition State. The association of fluorescently labeled S-peptide analogues with folded S-protein has allowed the transition state of a simple folding reaction to be characterized under strongly native conditions without reliance on extrapolation. The transition state is unstable by definition; an obvious barrier for bimolecular reactions is the translational entropy cost of bringing the reactants together. What other factors affect the free energy of the transition state for refolding? (a) It is stabilized by charge interactions at low salt concentrations, and these interactions are similar to those present in RNaseS*. (b) It has buried 55% of its sites for interaction with urea or GdmCl. (c) Nevertheless, it is not stabilized by specific side-chain interactions, as indicated by the small effect of mutations (small ϕ-values) on k_{on}. (d) The temperature dependence of the forward folding reaction suggests that the activated complex is collapsed and stabilized by hydrophobic interactions. (e) The rate-determining step of the reaction involves the diffusion together and collision of protein groups.

There are several important uncertainties remaining about the structure of the activated complex. The extent to which it is stabilized by helix formation is unknown, and it is not known whether the reaction is encounter-limited or folding-limited. There is evidence for an intermediate (I_r) which is populated at high concentrations of S-protein, and which may precede the rate-determining step in folding (preceding article). The lack of effect of mutations on k_{on} suggests that this intermediate is not stabilized by specific side-chain interactions, but its other properties are unknown. These issues must be resolved in future work.

ACKNOWLEDGMENT

We thank Dr. Stewart Loh for NMR characterization of H12A-1F and H12A/M13M′-1F, Dr. Douglas Laurents for valuable scientific discussions, and Dr. David Baker for preprints of his manuscripts.

REFERENCES

1. Doyle, R., Simons, K., Qian, H., and Baker, D. (1997) *Proteins: Struct., Func., Gen. 29*, 282−291.
2. Schellman, J. A. (1978) *Biopolymers 17*, 1305−1322.
3. Blackburn, P., and Moore, S. (1982) *The Enzymes 15*, 317−433.
4. Segawa. S., and Sugihara, M. (1984) *Biopolymers 23*, 2473−2488.
5. Scalley, M. L., and Baker, D. (1997) *Proc. Natl. Acad. Sci. U.S.A. 94*, 10636−10640.
6. Gómez, J., Hilser, V. J., Xie, D., and Freire, E. (1995) *Proteins: Struct., Func., Gen. 22*, 404−412.
7. Bryngelson, J. D., Onuchic, J. N., Socci, N. D., and Wolynes, P. G. (1995) *Proteins: Struct., Func., Gen. 21*, 167−195.
8. Karplus, M., and Weaver, D. L. (1976) *Nature 260*, 404−406.
9. Chrunyk, B. A., and Matthews, C. R. (1990) *Biochemistry 29*, 2149−2154.
10. Jacob, M., Schindler, T., Balbach, J., and Schmid, F., X. (1997) *Proc. Natl. Acad. Sci. U.S.A. 94*, 5622−5627.
11. Weast, R. C., Ed. (1974) *Handbook of Chemistry and Physics* Vol. 60, p D-270, CRC Press, Boca Raton, FL.
12. Graziano, G., Catanzano, F., Giancola, C., and Barone, G. (1996) *Biochemistry 35*, 13386-13392.
13. Chen, B., Basse, W. A., and Schellman, J. A. (1989) *Biochemistry 28*, 691−699.
14. Varadarajan, R., Connelly, P. R., Sturtevant, J. M., and Richards, F. M. (1992) *Biochemistry 31*, 1421−1426.
15. Gekko, K., and Timasheff, S. N. (1981) *Biochemistry 20*, 4667−4676.
16. Gekko, K., and Timasheff, S. N. (1981) *Biochemistry 20*, 4677−4686.
17. Wyckoff, H. W., Tsernoglou, D., Hanson, A. W., Knox, J. R., and Richards, F. W. (1970) *J. Biol. Chem. 245*, 305−328.
18. Richards, F. M., Wyckoff, H. W., Carlson, W. D., Allewell, N. M., Lee, B., and Mitsui, Y. (1971) *Cold Spring Harbor Symp. Quant. Biol. 36*, 34−43.
19. Jackson, S. E., elMasry, N., and Fersht, A. R. (1993) *Biochemistry 32*, 11270−11278.
20. Schreier, A. A., and Baldwin, R. L. (1977) *Biochemistry 16*, 4203−4209.
21. Sosnick, T. R., Jackson, S., Wilk, R. R., Englander, W., and Degrado, W. F. (1996) *Proteins: Struct., Func., Gen. 24*, 427−432.
22. Scalley, M. L., Yi, Q., Gu, H., McCormick, A., Yates, J. R., and Baker, D. (1997) *Biochemistry 36*, 3373−3382.
23. Schindler, T., and Schmid, F. X. (1996) *Biochemistry 35*, 16833−16842.
24. Alexander, P., Orban, J., and Byran, P. (1992) *Biochemistry 31*, 7243−7248.
25. Tan, Y., Oliveberg, M., and Fersht, A. R. (1996) *J. Mol. Biol. 264*, 377−389.
26. Myers, J. K., Pace, C. N., and Scholtz, J. M. (1995) *Protein Sci. 4*, 2138−2148.
27. Zwanzig, R. (1995) *Proc. Natl. Acad. Sci. U.S.A. 92*, 9801−9804.
28. Brouwer, A. C., and Kirsch, J. F. (1982) *Biochemistry 21*, 1320−1307.
29. Northrup, S. H., and Erickson, H. P. (1992) *Proc. Natl. Acad. Sci. U.S.A. 89*, 3338−3342.
30. Kramers, H. A. (1940) *Physica 7*, 284−304.
31. Haas, E., Katchalski-Katzir, E., and Steinberg, I. Z. (1978) *Biopolymers 17*, 11−31.
32. Teschner, W., Rudolph, R., and Garel., J. (1987) *Biochemistry 26*, 2791−2796.
33. Ansari, A., Jones, C. M., Henry, E. R., Hofrichter, J., and Eaton, W. A. (1992) *Science 256*, 1796−1798.
34. Waldburger, C. D., Jonsson, T., Sauer, R. T. (1996) *Proc. Natl. Acad. Sci. U.S.A. 93*, 2629−2634.
35. Janin, J. (1997) *Proteins: Struct., Func., Gen. 28*, 153−161.
36. D'Aquino, J. A., Gómez, J., Hilser, V. J., Lee, K. H., Amzel, L. M., and Freire, E. (1996) *Proteins: Struct., Func., Gen. 25*, 143−156.

37. Agashe, V. R., Shastry, M. C. R., and Udgaonkar, J. B. (1995) *Nature 377*, 754−757.
38. Chan, C., Hu, Y., Takahashi, S., Rousseau, D. L., Eaton, W. A., and Hofrichter, J. (1997) *Proc. Natl. Acad. Sci. U.S.A. 94*, 1779−1784.
39. Silow, M., and Oliveberg, M. (1997) *Proc. Natl. Acad. Sci. U.S.A.* 94, 6084−6086.
40. Ohgushi, M., and Wada, A. (1983) *FEBS Lett. 164*, 21−24.

BI972403Q